Helicon-excited electron paramagnetic resonance in $Hg_{1-x}Mn_xSe$

R. E. Kremer* and J. K. Furdyna†
Purdue University, West Lafayette, Indiana 47907
(Received 6 April 1987; revised manuscript received 11 September 1987)

We have used the techniques of microwave helicon transmission and helicon-excited electron paramagnetic resonance to study the behavior of the dynamic magnetic susceptibility in $Hg_{1-x}Mn_xSe$. The samples studied had manganese concentrations ranging from $x=0$ to $x=0.09$. This 9 at. % concentration forms an upper limit for the usefulness of the helicon technique. For low manganese concentrations ($x<0.005$), the EPR line is characterized by six hyperfine-split peaks, which yield a value of 60 G for the hyperfine splitting constant. As the amount of manganese is increased above 0.5 at. %, the six lines coalesce into a single broad peak, both the strength and width of which depend on the temperature and composition of the sample.

I. INTRODUCTION

$Hg_{1-x}Mn_xSe$ is a narrow-band-gap member of the family of materials referred to as diluted magnetic semiconductors (DMS). In these materials, a fraction x of the nonmagnetic cations of the host lattice have been replaced by magnetic ions (in the present case, Mn^{2+}).[1,2] The presence of the magnetic ions presents the possibility of a resonant interaction with circularly polarized microwaves when certain conditions are met. The electrical parameters of $Hg_{1-x}Mn_xSe$ are such that the application of a dc magnetic field allows these circularly polarized microwaves, known as helicons, to propagate with relatively little attenuation, thereby overcoming the problem associated with the classical skin depth.

The circular polarization admitted into the material depends on the sign of the free carriers. $Hg_{1-x}Mn_xSe$ presents a particularly attractive opportunity for the use of the helicon technique, in that there is a natural tendency for the material to form with a slight deviation from stoichiometry, leading to material that is strongly n type. When the carriers are electrons, the helicon polarization is the same as the sense of the precession of any localized paramagnetic dipoles which may be present in the material. Thus, for such an n-type plasma, when the conditions for electron paramagnetic resonance (EPR) are met, the helicons will react resonantly with the dipoles. The absence of holes in the material makes the interpretation of the results particularly reliable. The propagation of helicons provides a convenient, contactless method to study the electrical properties of the material.[3,4] The interaction of the helicons with magnetic dipoles, in conjunction with the electrical properties, allows us to measure both the real and imaginary parts of the dynamic susceptibility of the material directly.[5]

For manganese concentrations less than about 6 at. % (at liquid-helium temperatures), $Hg_{1-x}Mn_xSe$ is a zero-gap semiconductor. Above this value, a positive gap opens, and the helicon technique rapidly becomes inadequate as the number of carriers drops. We have found that $x=0.1$ roughly forms the upper limit for usefulness of the method.

Mullin *et al.* have previously examined a single sample of $Hg_{1-x}Mn_xSe$ containing 6 at. % manganese.[6] We have systematically extended this work to compositions both above and below $x=0.06$. For samples with x greater than about 0.005 the EPR is characterized by a single, broad peak, such as that described in Ref. 6. At lower concentrations, however, multiple peaks are observed, and a simple, two-level model of the dynamic magnetic susceptibility is no longer adequate. Fine and hyperfine interactions must be included.

In the next section, we first present a two-level model for the dynamic magnetic susceptibility, and then generalize it by including the fine and hyperfine interactions. The experimental apparatus and the details of the samples studied are described in Sec. III. Finally, we present and discuss our results in Sec. IV. For ease of presentation, we have divided the results into two groups: the low-x samples, where fine and hyperfine structures must be taken into account, and the intermediate-x samples, where the single line may be adequately described using a two-level system.

II. THEORETICAL BACKGROUND

$Hg_{1-x}Mn_xSe$ is an example of a gyrotropic medium, i.e., one that is rendered magnetically and electrically anisotropic by the application of a magnetic field. Helicon wave propagation in such a medium has been previously described (see, e.g., Ref. 5) and will not be discussed further. Earlier work on EPR in the diluted magnetic semiconductor family presented a simple model for the dynamic magnetic susceptibility based on a two-level spin system.[5-7] Rather than reproduce that development here, we will simply state the results.

In the framework of the Bloch model (see, e.g., Refs. 8 and 9) the susceptibility may be written

$$\chi'_{\pm}=\frac{-\chi_0\omega_0(\omega\mp\omega_0)T_2^2}{1+(\omega\mp\omega_0)^2T_2^2}\ ,$$
$$\chi''_{\pm}=\frac{\pm\chi_0\omega_0T_2}{1+(\omega\mp\omega_0)^2T_2^2}\ , \tag{1}$$

where single and double primes denote real and imaginary parts of the susceptibility, respectively, the $\pm$ subscripts refer to the two circular polarizations, χ_0 is the static magnetic susceptibility, ω is the microwave angular frequency, $\omega_0=geB/2m$ is the Larmor precession frequency, and T_2 is the spin-spin relaxation time. This model of the dynamic magnetic susceptibility corresponds to a simple two-level spin system. While such a form is useful for the understanding of EPR dynamics, it becomes inadequate for discussing the EPR interaction in samples that are magnetically very dilute. In the dilute case we must also include the hyperfine interaction between the outer electrons of the Mn^{2+} ion and its nuclear spin, and the fine interaction between the outer electrons and the crystal field of the host lattice.

The outer electron configuration of a manganese atom consists of $3d^5 4s^2$. When doubly ionized, the two s electrons become delocalized in the valence band, leaving only the five $3d$ electrons bound to the ion. Since a d shell may contain up to ten electrons, Hund's rules indicate that the lowest-energy configuration for the half-full Mn^{2+} $3d$ shell consists of all five electrons unpaired. The five electrons then contribution a net spin of $\frac{5}{2}$ to the ionic magnetic moment. This leads to six possible spin orientations for the ion: $M_J=\pm\frac{5}{2},\pm\frac{3}{2},\pm\frac{1}{2}$, with the energy levels being degenerate in zero magnetic field. The application of a magnetic field splits the system into six equally spaced levels separated by A, the hyperfine-splitting constant. Since transitions between the levels are governed by the selection rule $\Delta M_J=\pm1$, all possible transitions correspond to the *same* energy.

If we now place the manganese ion into a cubic lattice, the crystal field breaks the zero-field degeneracy. The single sixfold-degenerate level splits into a quadruplet state at $+a$ and a doublet state at $-2a$, where a is the fine-structure-splitting constant. The application of a magnetic field will split the two levels further into a total of six levels, removing all degeneracy, as shown in Fig. 1. As before, the allowed transitions correspond to $\Delta M_J=\pm1$. However, since the levels are now no longer equally spaced, each possible transition ($-\frac{5}{2}\leftrightarrow-\frac{3}{2}$, $-\frac{3}{2}\leftrightarrow-\frac{1}{2},\ldots,\frac{3}{2}\leftrightarrow\frac{5}{2}$) corresponds to a slightly different energy and the EPR spectrum exhibits fine structure consisting of five lines, as shown in Fig. 1.

Since the fine-structure interaction is due to the crystal field, the amount of splitting in the spectrum is strongly dependent on the orientation of the applied magnetic field with respect to the crystal axes. As is well known, the amplitude of the splitting is largest when the applied field is in the [110] plane along the [100] axis and vanishes at about 30° from the [100] axis (see, e.g., Ref. 10).

The hyperfine interaction arises from the coupling between the spin of the $3d^5$ electrons and the nuclear spin,

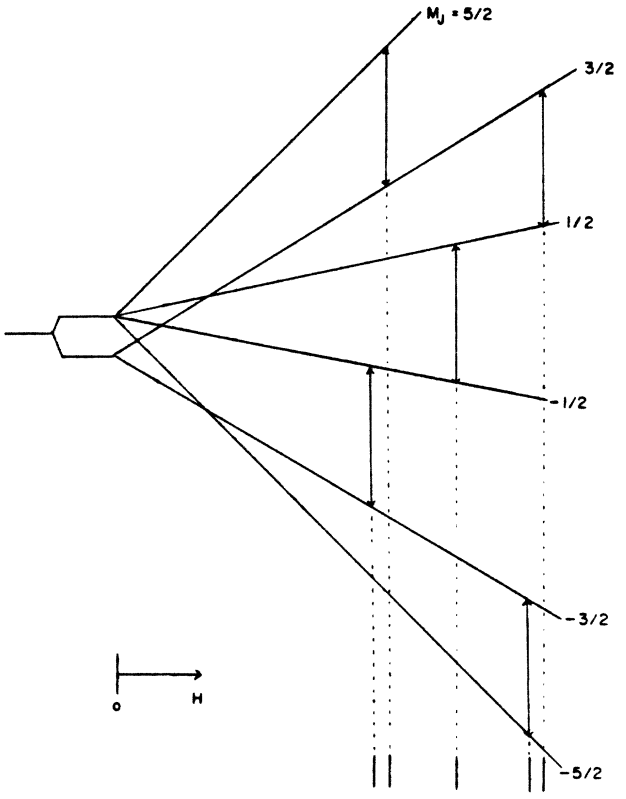

FIG. 1. Fine-structure splitting of the Mn^{2+} $3d^5$ level in a magnetic field. The six levels lead to five lines in the EPR spectrum.

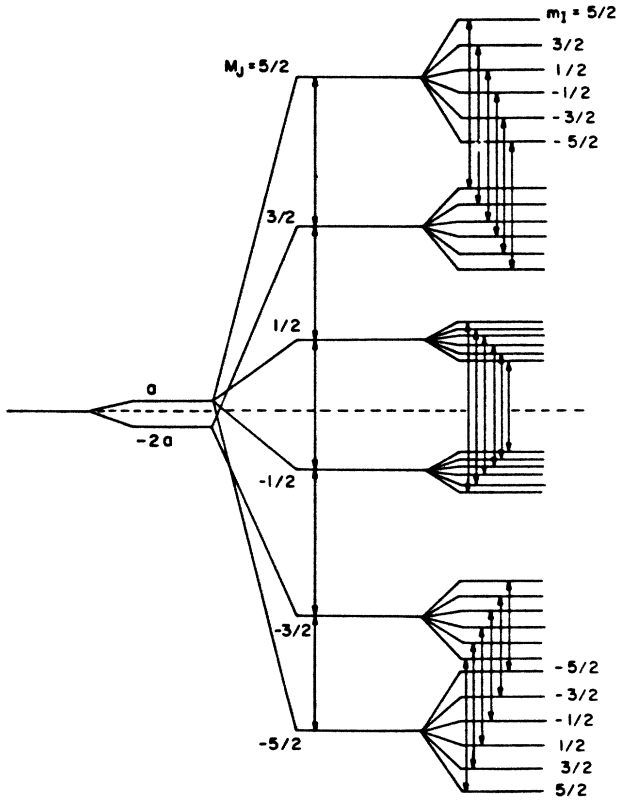

FIG. 2. Energy levels of the Mn^{2+} ion in a magnetic field showing fine and hyperfine splitting. Transitions corresponding to $\Delta M_J=1$, $\Delta m_I=0$ are shown. Transitions from $M_J=-\frac{3}{2}\leftrightarrow-\frac{1}{2}$ and $\frac{1}{2}\leftrightarrow\frac{3}{2}$ are omitted for clarity.

which in the case of the manganese ion has the value $m_I=\frac{5}{2}$. This interaction splits each fine-structure level into six levels corresponding to the six possible values of the nuclear spin $m_I(=\pm\frac{5}{2},\pm\frac{3}{2},\pm\frac{1}{2})$. This additional splitting is shown in Fig. 2. Transitions between these levels are governed by the hyperfine selection rules which require $\Delta m_I=0$. With each of the five fine-structure lines being hyperfine split into six lines, the total EPR spectrum consists of a maximum of 30 lines. Although we do not have an analytic expression for χ including the contributions of the fine and hyperfine splitting, we can use a phenomenological picture where

$$\chi=\sum_i \chi_i \ , \tag{2}$$

with each individual χ_i having the Bloch form of Eq. (1) but with a slightly different Larmor frequency ω_0, such that

$$\hbar\omega_{0i}=\Delta E_i \ , \tag{3}$$

where ΔE_i is the energy difference for a particular transition allowed by the selection rules described above.

III. EXPERIMENTAL CONSIDERATIONS

The microwave transmission experiments were performed in the Faraday geometry (magnetic field parallel to direction of propagation) using a 35-GHz Rayleigh interferometer bridge. The apparatus, shown in Fig. 3, has been described in detail elsewhere.[5,6] Samples were made by slicing thin disks (thickness of about 0.5 mm) from the ingot. They were mounted on an iris with the edges sealed with highly conductive silver paste to prevent microwave leakage around the samples. The entire sample holder was then placed in the bore of a 6-T superconducting magnet.

The $Hg_{1-x}Mn_xSe$ ingots were grown from the melt using a vertical Bridgman process. As-grown crystals tend to be strongly n type due to a natural tendency for this material to form with a stoichiometric excess of the metallic ions. To reduce the electron concentration to a level where conditions for helicon propagation are satisfied,[1,2] slices were annealed for 48 h at 200 °C in dynamic vacuum. Since, as in the case for other HgTe-based pseudobinary compounds,[11,12] the composition varies strongly along the length of the ingot, the composition had to be determined for each sample used in the investigation. For samples with greater than 1% manganese, this composition analysis was done using density measurements. The density technique lacks sufficient sensitivity, however, for the lower concentrations. For samples with less than 1% manganese, the composition was calculated from the magnitude of the static magnetic susceptibility, assuming noninteraction among the spins present. This measurement is described more fully in the next section.

The electrical parameters of the samples were obtained from the microwave transmission, using Rayleigh interferogram data at fields well away from the paramagnetic resonance. The dependence of the helicon phase on magnetic field gives a measure of the electron concentration, while the mobility can be calculated from the amplitude dependence. The details of the calculations have been described previously.[7] Table I lists composition, electron concentration, and electron mobility for the samples used. Data is shown for 4.2 K and "high temperature," where the latter refers to measurements made between 75 and 95 K, depending on the sample. Note that the electron concentration remains constant over this temperature range. However, there is a small, but systematic decrease in the mobility as the samples are heated. The drop in mobility measured using the helicon method agrees with dc electrical measurements made on this material.[13,14]

The mobilities of all of the samples used in this investigation were comparable. Significant differences appeared in the electron concentration, however. The low number of carriers for the 7- and 9-at. % samples can be explained by noting that the band gap of $Hg_{1-x}Mn_xSe$ opens for manganese concentrations above about 6 at. % at 4.2 K. This opening of the gap results in a significant drop in the electron concentration. The remainder of the samples, with x values ranging from 0 to 0.05, were zero-gap materials. The variation in carrier concentration among these samples is somewhat more surprising, but is probably due to slight variations in growth and annealing conditions, especially the latter.

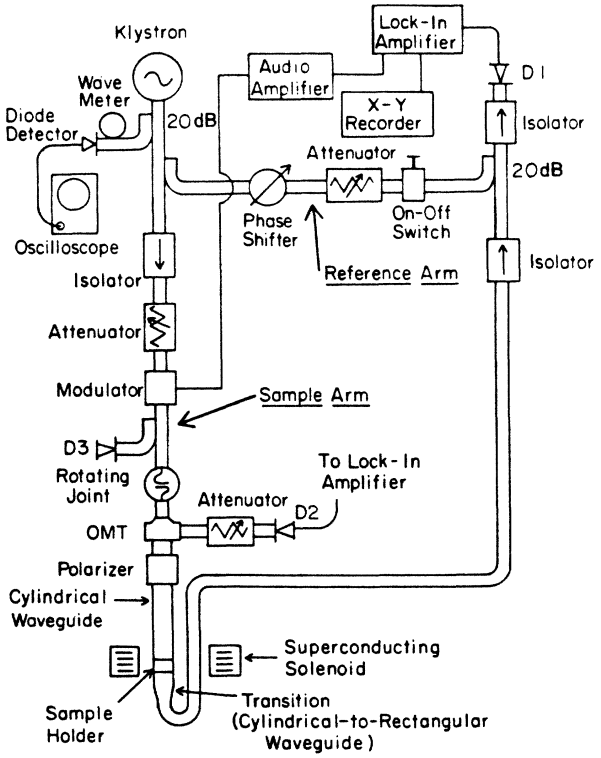

FIG. 3. Block diagram of the microwave spectrometer used in the experiments.

TABLE I. Electrical properties of the HgMnSe samples used in this investigation.

Sample	Mn^{2+} Conc. (x)	4.2 K n ($\times 10^{23}/m^3$)	4.2 K μ (m^2/Vs)	High T n ($\times 10^{23}/m^3$)	High T μ (m^3/Vs)
S 25 *B*2	0	0.9	11.6	1.3	10.6
S 32 *B*2	5×10^{-5}	8.7	7.6		
S 27 *C*2	3×10^{-4}	2.5	9.3	2.4	7.2
S 33 *D*2	8×10^{-4}	1.6	7.4		
S 33 *B*2	3×10^{-3}	5.2	8.5	5.3	7.4
S 34 *B*1	7×10^{-3}	1.8	9.6	1.7	9.1
S 14 *A*	2×10^{-2}	1.0	7.0	1.0	7.0
S 19 *B*3	3×10^{-2}	3.6	9.5	3.6	8.0
S 18 *E*9	5×10^{-2}	2.4	10.5	2.1	7.4
S 23 2 *A*	7×10^{-2}	0.2	7.0	0.2	2.7
2194 *D*2	9×10^{-2}	0.4	4.4	0.4	2.3

IV. RESULTS AND DISCUSSION

This section presents the results of our study of helicon-excited EPR in $Hg_{1-x}Mn_xSe$. We have systematically examined samples containing no manganese, very little manganese, and moderate amounts (up to 9 at. %) of manganese to see how the behavior of the dynamic magnetic susceptibility changes with manganese concentration. To facilitate discussion of the results, we have divided this section into three parts. The first describes the susceptibility for samples with $x < 0.005$. For these samples, fine and hyperfine structure must be taken into account in order to adequately explain the data. The second part of this section discusses data obtained from material containing larger amounts of manganese. Here, the simple two-level model discussed earlier[6] accurately described our results. In the final part of this section, we present the results of an analysis of the linewidth of the resonance. The width provides a direct measure of T_2, the spin-spin relaxation time.

A. Low Mn^{2+} concentrations ($x < 0.005$)

When only a small fraction of the mercury ions have been replaced by manganese ions, several assumptions can be made. The first assumption concerns the location of the manganese ions in the fcc lattice. In the related material $Hg_{1-x}Mn_xTe$ at manganese concentrations of about 3 and 6 at %, measurements of the specific heat by Nagata *et al.* could be best explained by assuming a nonrandom distribution of ions.[15] In particular, the results indicated a tendency for the manganese ions to form clusters, whereas a random distribution would have a large fraction of them with only mercury nearest neighbors. Since the manganese concentrations discussed in this section are at least an order of magnitude lower, however, we will continue to assume a random distribution. Nearly all of the manganese ions (95% or more) will have no other manganese ions as nearest neighbors.[16]

We will also assume that these isolated ions are independent of each other. Exchange effects between manganese ions have been shown to be important (see, e.g., Refs. 17 and 18), but only at higher concentrations. Each ion can be assumed to be an isolated paramagnet in the HgSe host lattice. This point will be discussed further below, as it is used to calculate the actual composition of these very dilute samples.

The most striking aspect of data obtained from the low-x samples is the presence of six well-resolved hyperfine lines in the EPR spectrum. Measurements of the splitting between the lines yields a value of 60 G for A, the hyperfine-splitting constant. This value agrees well with those obtained from EPR measurements of Mn^{2+} in CdTe, both conventional,[19,20] and our own.[21]

While the hyperfine interaction was readily visible in the low-x sample, fine-structure splitting remained unresolved in all of our EPR data from $Hg_{1-x}Mn_xSe$. Samples with differing concentrations of manganese were tried, and several different orientations of the magnetic field with respect to the crystal axes were used.

We tentatively ascribe the absence of fine structure to the large number of highly mobile electrons that are present in HgSe-based alloys. Zimmermann *et al.* have seen similar behavior in the case of dilute alloys of magnetic ions in metals (e.g., gadolinium ions in magnesium)[22] where the electron concentration is, of course, very large. Due to a spin-spin exchange interaction between the localized electrons comprising the Gd^{3+} ion and the conduction electrons, the EPR fine structure collapses to a single line. In this exchange narrowing process, encounters with the free electrons cause the satellite lines to weaken or disappear completely.

An alternative explanation is also due to the presence of a large number of conduction electrons in $Hg_{1-x}Mn_xSe$. Since the electrons are highly mobile, their random paths may tend to screen or smear out the crystal fields as perceived by the manganese ions. Thus, much higher magnetic fields may be necessary before fine structure can be observed in this material.

Regardless of the exact reason for the disappearance of the fine structure, we feel that it must be connected to the large number of electrons present. This hypothesis is supported by the fact that in insulating $Cd_{1-x}Mn_xTe$ (Ref. 21) and in undoped $Hg_{1-x}Mn_xTe$ (where n is on the order of $2\times10^{15}/cm^3$),[21] samples with equally low manganese concentrations exhibit well-resolved fine structure in addition to the hyperfine structure. The absence of fine structure in $Hg_{1-x}Mn_xSe$ appears to be an interest-

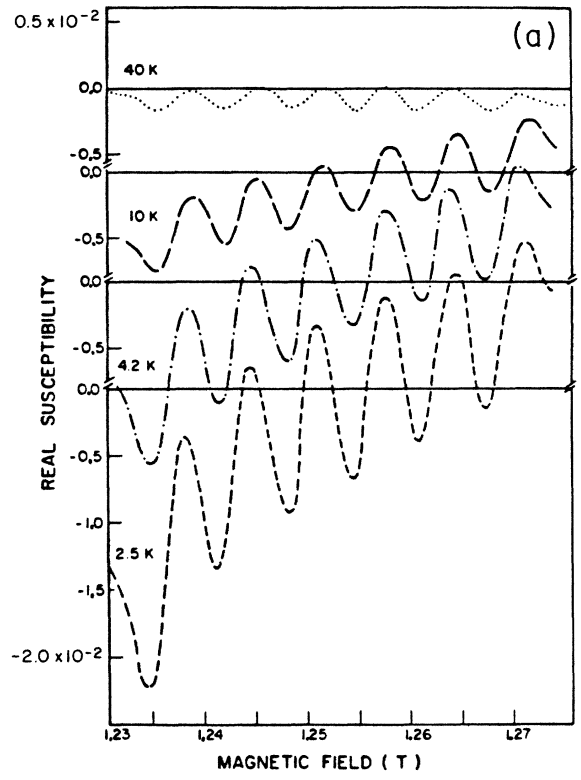

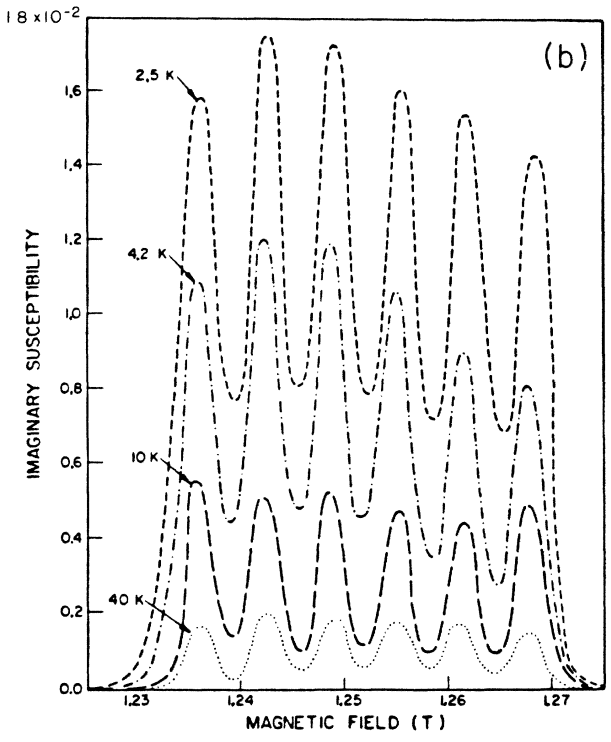

FIG. 4. (a) Real part of the dynamic magnetic susceptibility for $Hg_{1-x}Mn_xSe$ with $x=0.0003$ at several temperatures. The curves have been displaced vertically for clarity. (b) Imaginary part of the susceptibility for the same sample.

ing example of where an electrical property, the free-carrier concentration, modifies a magnetic one, the dynamic magnetic susceptibility.

Once the electrical parameters have been determined from the parts of the interferogram away from EPR, they may be used to quantitatively calculate the real and imaginary parts of the dynamic magnetic susceptibility.[5] In Figs. 4(a) and 4(b) we show the real and imaginary parts of the susceptibility, respectively, for a sample with $x=0.0003$ with the dc field applied along the [100] direction at temperatures from 2.5 to 40 K. Neglecting the unresolved fine structure, the hyperfine peaks of χ''_+ may be represented as the sum of six terms, each behaving according to the Bloch equations and each having a different nuclear quantum number. Equation (1) for χ'' then becomes [in the form of Eq. (2)]

$$\chi''_+=\frac{\chi_0}{6}\sum_{m_I=-5/2}^{5/2}\frac{(\omega_0)_{m_I}T_2}{1+[\omega-(\omega_0)_{m_I}]^2T_2^2}\ , \tag{4}$$

where

$$(\omega_0)_{m_I}=ge(B+m_I A)/2m_0\ . \tag{5}$$

Here A is the hyperfine-splitting constant. Equation (4) for χ''_+ assumes that the magnetization has not saturated, i.e., that we are still in the linear portion of the M versus B curve, where M is the magnetization of the sample. Note in Fig. 4(b) that even at this low value of x the individual lines broaden as the temperature falls. While the resonance is stronger at 2.5 K, the hyperfine peaks in Fig. 4(b) are only about 50% resolved. At 10 K, in contrast, although the individual lines are weaker, they are about 80% resolved. As the temperature is raised further, the resolution continues to improve, but the amplitude decreases until the entire feature vanishes at about 90 K.

Integrating χ''_+ over B, or equivalently over ω_0, yields a constant times χ_0 for all the spins, independent of T_2. From Eq. (1) we have

$$\int_{-\infty}^{\infty}\chi''_+dB\rightarrow\int_{-\infty}^{\infty}\frac{\chi_0\omega_0T_2}{1+(\omega-\omega_0)^2T_2^2}d\omega_0=\pi\omega\chi_0$$

$$=6.91\times10^{11}\chi_0 \tag{6}$$

for our frequency of 35 Ghz. Thus the area under the χ'' curves in Fig. 4(b) is a direct measure of χ_0 for that given temperature. If we assume that the ions are noninteracting (which is a good assumption for these very low Mn^{2+} concentrations), the static susceptibility is given by

$$\chi_0=\frac{N_s\mu_0\mu_{\rm eff}^2}{3k_BT}\ , \tag{7}$$

where N_s is the number of spins per unit volume, μ_0 and k_B are the permeability of free space and the Boltzmann constant, respectively, T is the temperature, and $\mu_{\rm eff}$ is the effective magnetic moment of the manganese ion, which we take to be $\mu_{\rm eff}=5\mu_B$ (five unpaired electrons,

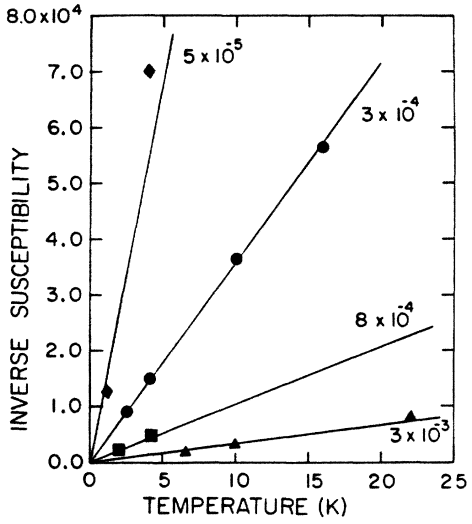

FIG. 5. Temperature dependence of the inverse static susceptibility for several low concentration samples. The straight lines indicate Curie-type behavior.

each contributing one Bohr magneton). So once we have found χ_0 by integrating, Eq. (7) can be used to calculate N_s and thus x, the mole fraction of manganese in the crystal. This is very useful for the low concentrations, since other methods of determining compositions at such low values of x (e.g., density measurement) become unreliable. Having a method to determine the manganese content in a particular sample is especially important in Bridgman crystals of the mercury compounds, where longitudinal concentration gradients are disadvantageously high.[11,12] Figure 5 summarizes the temperature dependence of the static susceptibility for the low-Mn^{2+}-concentration samples. The straight lines imply Curie-law behavior for these concentrations, in keeping with our earlier assumption of noninteracting spins.

Using the microwave helicon transmission technique we were able to observe the EPR with its six hyperfine peaks in samples with manganese concentrations as low as $x = 5 \times 10^{-5}$. For this lowest concentration sample, the resonance was barely measurable at 4.2 K, and only by reducing the temperature to about 1.3 K could reliably accurate data be taken. To examine lower Mn^{2+} concentrations, thicker samples would be needed, which would result in less microwave transmission. A more sensitive detector and/or the use of quarter-wave plates[23] would then be necessary to detect the signal.

One additional item of interest should be noted in this section. In the discussion of helicon propagation referred to above,[5] it was pointed out that the strength of the EPR absorption was actually enhanced by the presence of a large number of electrons. As was mentioned in Sec. III, our $Hg_{1-x}Mn_xSe$ samples were annealed in dynamic vacuum, which acts to lower the electron concentration. This material, however, disadvantageously tends to lose its annealed properties, often quite rapidly. In one sample, the electron concentration increased by a factor of 4 overnight. Figure 6 shows the EPR interferogram both before and after this change in electron concentration. The increased value of n is evidenced by the reduced helicon period of the interferogram in Fig. 6(b). Since the number of spins remains unchanged, the measured susceptibility must be the same for the two traces. Note, however, that the strength of the resonance is dramatical-

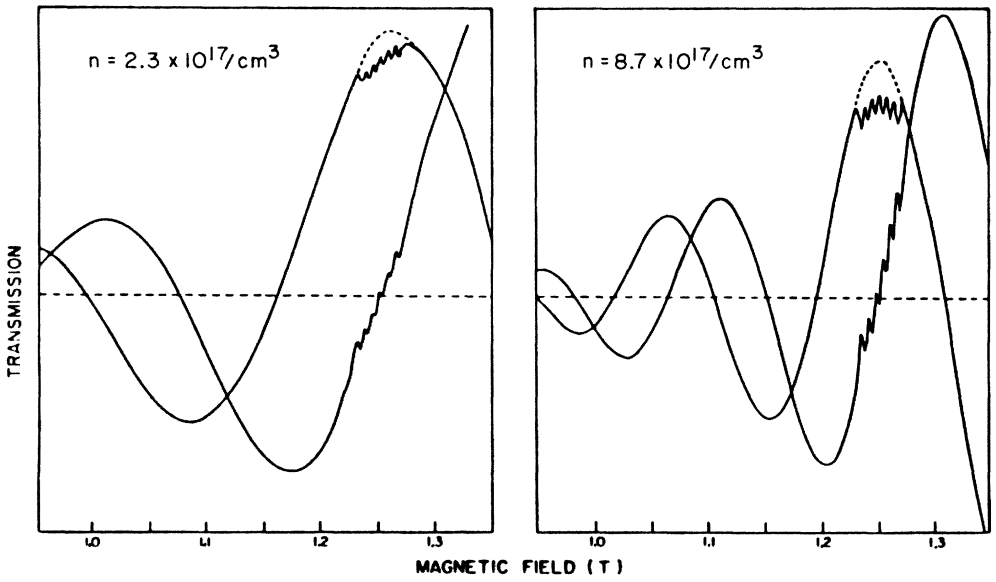

FIG. 6. Rayleigh interferograms for a sample with $x = 0.0003$ taken on two consecutive days showing the enhancement of EPR due to an increase in the electron concentration. The electron concentration in (a) is 2.3×10^{17} cm^{-3}, and in (b) has increased to 8.7×10^{17} cm^{-3} as evidenced by the decreased helicon period.

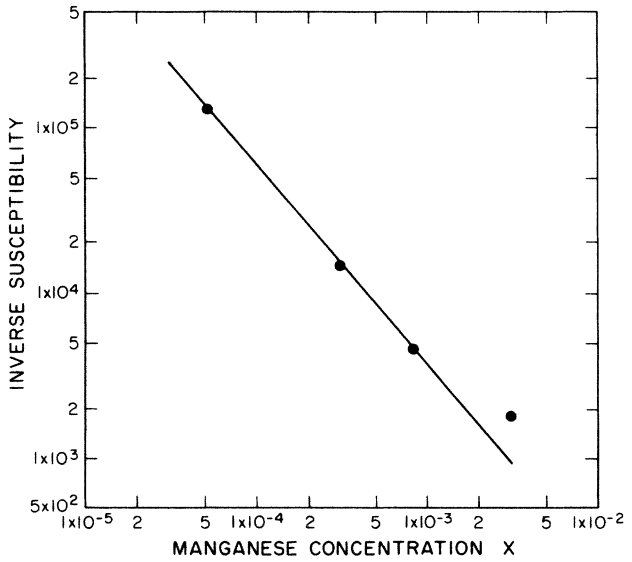

FIG. 7. Log-log plot of inverse static susceptibility as a function of manganese concentration for the low-x samples.

ly increased in the case corresponding to the larger value of n. We believe that this is the first time that this enhancement of EPR by an increase in the electron concentration has been unambiguously demonstrated experimentally.

Finally, we note that in this low manganese-concentration range, the magnetic susceptibility is directly proportional to the number of spins present in the samples. The inverse of the static susceptibility is shown as a function of manganese concentration in Fig. 7. With the exception of the 0.3-at. % sample, the data shown were taken at 4.2 K. Since this sample was measured at 6.5 K, it is not surprising that the susceptibility is somewhat smaller than expected. In this low-x range, the antiferromagnetic interaction between manganese spins is not readily apparent. But even in this dilute limit, the line-broadening process that will later (at higher values of x) become completely dominant is observable. As has already been noted, the hyperfine lines broaden (as evidenced by a decrease in resolution) as the temperature decreases.

B. Intermediate-Mn^{2+}-concentration samples ($0.005 < x < 0.10$)

As x is increased above 0.005, the six hyperfine lines broaden to form a single line due to interactions between the manganese ions. With further increase in the manganese content, the broadening becomes very dramatic, and is accompanied by a gradual decrease in the resonance strength. Since $Hg_{1-x}Mn_xSe$ samples with up to about 10 at. % manganese still contain a large number of highly mobile electrons, we can continue to employ the method of helicon-excited EPR to study the dynamic magnetic susceptibility in these samples. At concentrations near 10 at. %, however, the resonance at low temperatures becomes too broad and too weak for quantitative measurement, thus establishing a practical limit for the usefulness of the helicon method.

From Rayleigh interference data, the real and imaginary parts of the dynamic magnetic susceptibility can be calculated.[5] We show calculated values for a sample with 2 at. % manganese at several temperatures in Fig. 8. As the temperature is raised above 4.2 K, the resonance line both weakens and narrows in a manner similar to that observed by Mullin *et al.* for a 6-at. % sample.[6] The weakening of the resonance with increasing temperature is due to the normal temperature dependence of χ_0. The large linewidth at low temperatures indicates that the exchange interaction between the manganese ions is already quite strong at $x = 0.02$. This exchange interaction is formally represented through the spin-spin relaxation time T_2 in Eq. (1) and will be further discussed below. The EPR line is seen to be Lorentzian in nature, with the dispersive effects (real part of the susceptibility) extending for several kG from the center of the resonance while the absorptive effects (imaginary part) have a considerably narrower range.

By fitting Eq. (1) for χ_+ to our data (we fit both the real and imaginary parts simultaneously), we get values of χ_0 and T_2. In Figs. 8(a) and 8(b) the points represent the measured values of the real and imaginary parts of the dynamic magnetic susceptibility, obtained from the Rayleigh data and the solid lines are the "best-fit" theoretical values of χ' and χ'' obtained by using the same parameters χ_0 and T_2 for both the real and imaginary parts.

We have identified the parameter χ_0 as the dc or static magnetic susceptibility. Usually static susceptibility measurements are made at fields of a few gauss, whereas ours are made at 1.25 T. Thus our susceptibility must, strictly speaking, be understood as a measure of the magnetization ($M = \chi_0 H$) at that large field, and corresponds to the low-field χ_0 only in the range where M is linear with H. The inverse of our χ_0 is shown in Fig. 9 as a function of temperature for three values of x. Comparison with Fig. 5 reveals that, while in the case of very low manganese concentrations we had seen Curie-type behavior indicating little ionic interaction (Fig. 5), for these higher concentrations there is a significant amount of interaction between the ions. This interaction is evidenced by the characteristic downturn in the inverse susceptibility at low temperature which is seen in all DMS susceptibility studies.[2] This feature has been ascribed to the previously mentioned tendency of the ions to form spin clusters as the temperature is decreased.[24]

In the extremely dilute manganese concentration range discussed in the preceding section, we recall that the susceptibility was directly proportional to x. As more manganese was added, both χ_0 and χ_+ increased. Above about 2 at. % manganese, however, the interaction between the ions becomes increasingly important, and due to the antiferromagnetic nature of this interaction, χ_0 no longer increases as fast as x. Since, in addition, the increase of x is accompanied by a broadening of the resonance, this leads to the behavior also seen in Fig. 9, illustrating that this bowing effect increases with manganese concentration above about 2 at. %. The effect becomes

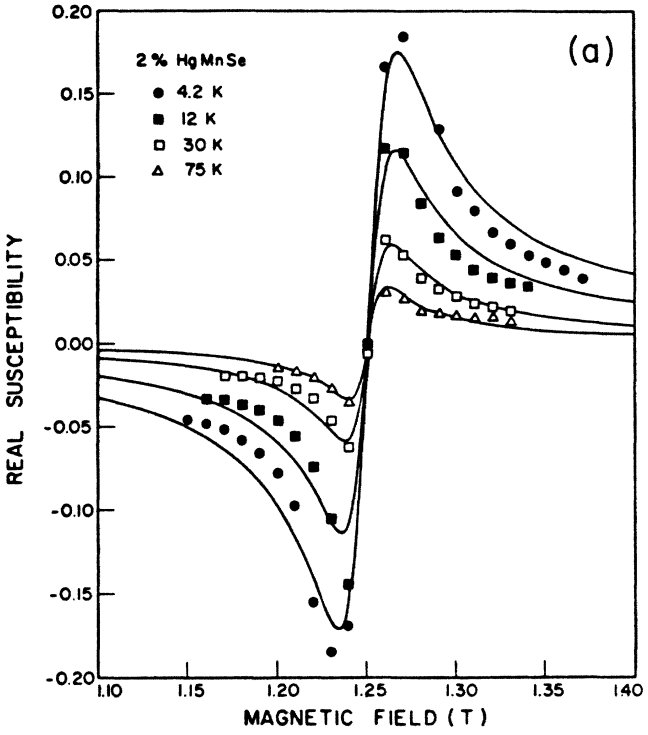

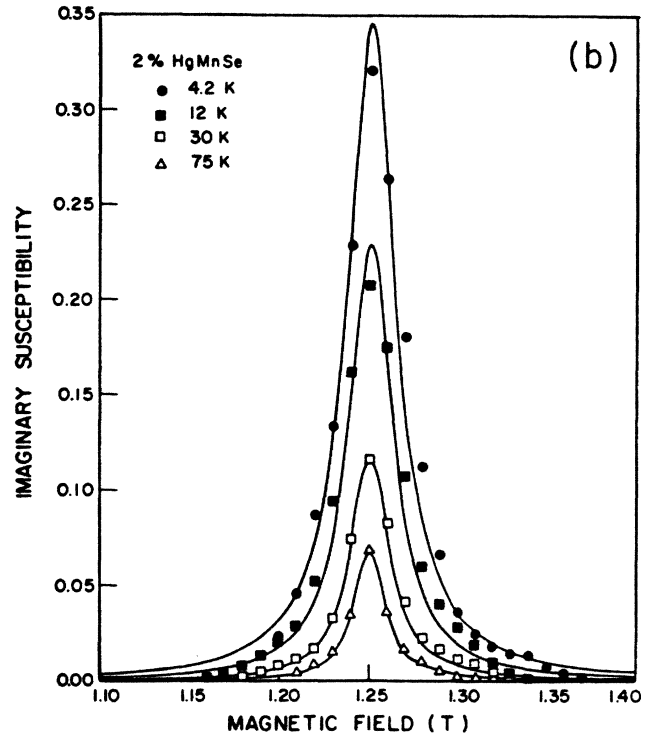

FIG. 8. (a) Real part of the dynamic magnetic susceptibility for $Hg_{1-x}Mn_xSe$ containing 2 at. % manganese measured at several different temperatures. The points are measured data and the lines are the best fits obtained by fitting the real and imaginary parts of the susceptibility simultaneously. (b) Imaginary part of the susceptibility for the same sample.

more noticeable as the temperature is increased. Note the sharp contrast between this behavior for intermediate-concentration samples and that shown in Fig. 7 for the very-dilute limit.

When the manganese concentration is increased above 6 at. %, $Hg_{1-x}Mn_xSe$ undergoes a zero-gap semiconductor to open-gap semiconductor transition. This increase of x is accompanied by a rather rapid disappearance of the helicon-excited EPR, so that in the open-gap range the helicon method becomes progressively less useful. This behavior is caused by three cooperating factors. Above a certain concentration (roughly $x=0.02$), as more manganese is added, the antiferromagnetic interaction between the ions tends to lower the effective value of χ_0, thus making the resonance weaker. In addition, as x increases, the relaxation time T_2 decreases, resulting in broader lines. Finally, as was illustrated in Fig. 6, the intensity of EPR observed by the helicon method is proportional to $\sqrt{n}$, where n is the electron concentration, and in the open-gap region ($x>0.06$) the electron concentration is considerably lower (see Table I). Thus the combination of a weak, broad form of χ_+ and a lower electron concentration leads to EPR signals that are barely discernible using the helicon method. Figure 10 shows the resonance for a 9-at. % sample at 4, 8, 40 K. There is a sharp contrast between the low-temperature behavior in

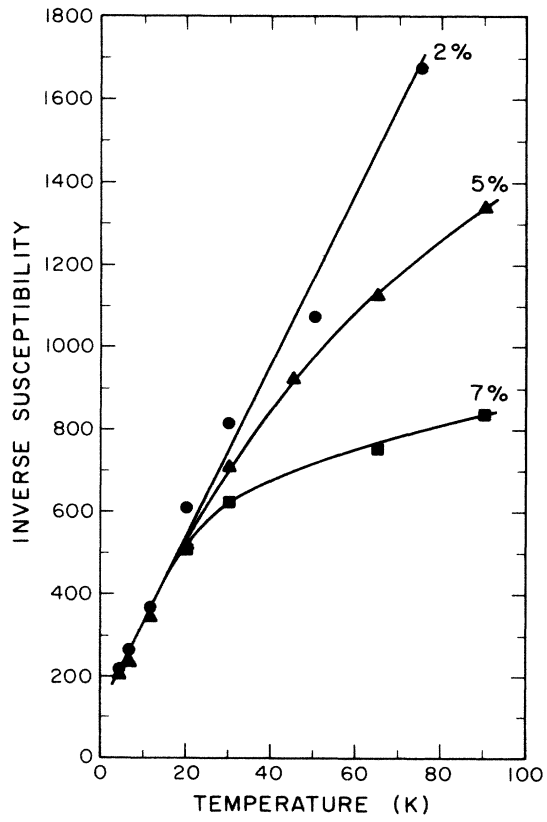

FIG. 9. Inverse static susceptibility shown as a function of temperature for several samples in the intermediate-x range. The lines are guides for the eyes.

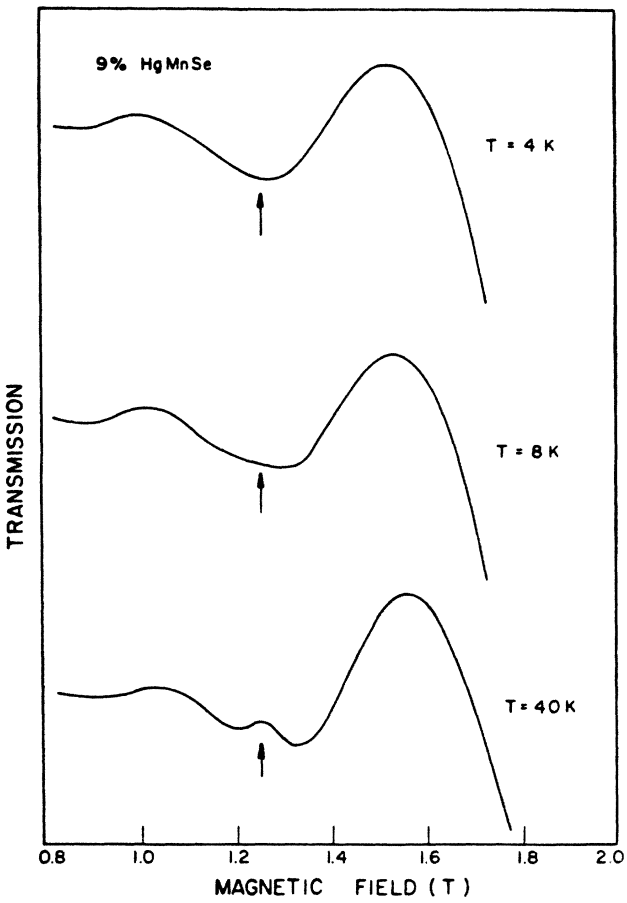

FIG. 10. Rayleigh interferogram traces for a sample containing 9 at. % manganese taken at 4, 8, and 40 K. The position of the resonance is shown by the arrow.

Fig. 10 and that shown by samples with 1–2 at. % manganese where the microwave interference signal is totally extinguished by EPR. In addition, the analysis of the helicon EPR effect for the higher concentrations is complicated by the fact that the width of the EPR line is now comparable to the helicon period. We conclude, therefore, that the helicon method of exciting and measuring EPR becomes unreliable at low temperatures for the open-gap materials. EPR measurements on powder samples[25] may prove to constitute a more practical technique for the study of this concentration range.

C. Linewidth analysis

We have concentrated primarily on the strength of the resonance in the above discussion of EPR. We now briefly mention the linewidth of the resonance. The width of the resonance in $Hg_{1-x}Mn_xSe$ depends on both the Mn^{2+} concentration and the temperature, and provides a direct measure of T_2, the spin-spin relaxation time.[7] For the low concentrations, where hyperfine splitting is present, the individual lines are separated by about 60 G (with the width of each individual line being less than the separation), leading to an EPR spectrum of total width slightly greater than 350 G. As the amount of

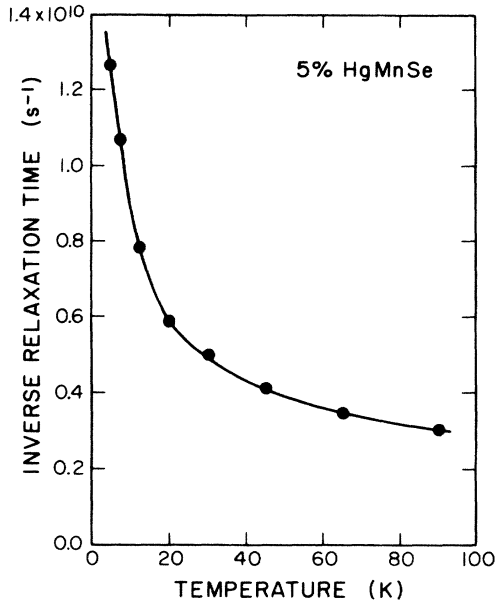

FIG. 11. Inverse spin-spin relaxation time ($1/T_2$) shown as a function of temperature for a sample containing 5 at. % manganese.

manganese is increased, the individual lines become broader than their separation, and the whole spectrum coalesces into a single line whose width depends strongly on the temperature, and can be very much wider than 350 G.

At high temperatures, however, this single line narrows dramatically, indicating a sharp increase in T_2. The

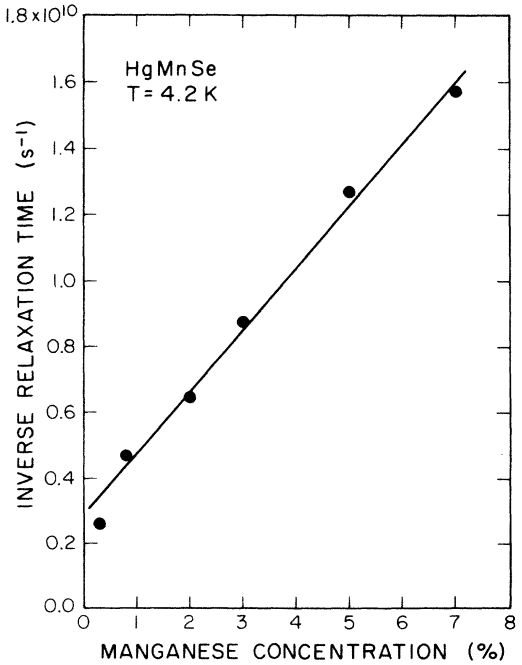

FIG. 12. Inverse spin-spin relaxation time ($1/T_2$) measured at 4.2 K for $Hg_{1-x}Mn_xSe$ shown as a function of manganese concentration x.

width of the line can actually be less than the 350-G width of the overall hyperfine spectrum. We ascribe this behavior to motional narrowing.[9] An example of this narrowing is shown in Fig. 11, where we plot the inverse of T_2 as a function of temperature for a sample with 5 at. % manganese. It should be pointed out that this is not an effect observed only in $Hg_{1-x}Mn_xSe$. A similar large increase in linewidth with decreasing temperature has been reported in all other members of the diluted magnetic semiconductor family as well.[26]

As has also been observed in other diluted magnetic semiconductors, the width of the EPR line increases as the manganese concentration is increased at a constant temperature. This increase is shown in Fig. 12, where the inverse of T_2 measured at 4.2 K is plotted against the manganese concentration. The dependence appears to be nearly linear with x.

V. CONCLUSIONS

We have studied helicon-excited EPR in a wide variety of $Hg_{1-x}Mn_xSe$ samples, systematically covering manganese concentrations from $x=0.000\,05$ to $x=0.1$. Since the resonance becomes weaker as the number of spins is decreased, this concentration of $x=0.000\,05$ appears to form the lower limit of detectability. The upper limit on manganese concentration for this technique is about $x=0.1$, where the difficulty stems from a combination of antiferromagnetic interaction among spins, wide resonances, and decreasing numbers of free electrons.

For concentrations of less than about 0.5 at. %, a simple two-level model of the manganese spin systems is inadequate to describe the results. The resonance in these low-x samples is characterized by six hyperfine-split lines, separated by about 60 G. We did not observe fine-structure splitting in any of the samples we measured, leading to the conclusion that the fine-structure interaction is suppressed by the large concentration of electrons present in HgSe-based materials. For the low-Mn^{2+} samples, the magnetization has a Curie-law temperature dependence and is directly proportional to the manganese concentration.

As the manganese concentration is increased above about 0.5 at. %, the hyperfine lines coalesce into a single peak, the behavior of which is similar to that reported earlier.[6] In this regime, the magnetization increases at low temperatures with stronger than a Curie-law temperature dependence. This dependence leads to a downturn in the inverse susceptibility at low temperatures that appears to be characteristic of all diluted magnetic semiconductors. For these intermediate-x samples, antiferromagnetic exchange among manganese ions becomes important, causing susceptibility to increase at a slower rate than x.

The width of the resonance varies strongly with both temperature and sample composition. For a given manganese concentration, the linewidth decreases dramatically as the temperature is raised, implying a rapidly increasing spin-spin relaxation time. In addition, the resonance linewidth appears to vary linearly with manganese concentration when the measurements are made at a constant temperature.

ACKNOWLEDGMENTS

This work was partially supported by the National Science Foundation through Grant Nos. DMR-83-16988 and ECS-84-02080, U.S. Defense Advanced Research Projects Agency/Office of Naval Research and the Oregon Graduate Center Solid State Consortium. The authors would like to thank Dr. J. E. Sansonetti, Dr. N. Samarth, and Dr. D. D. Kirchhofer for useful discussions.

---

*Present address: Crystal Specialties, Intl., 2853 Janitell Rd., Colorado Springs, CO 80906.

†Present address: Notre Dame University, Notre Dame, IN 46556.

[1]R. R. Galazka, in *Proceedings of the 18th International Conference on the Physics of Semiconductors,* edited by O. Engstrom (World-Science, Singapore, 1987), p. 1717.

[2]J. K. Furdyna, J. Appl. Phys. **53**, 7637 (1982).

[3]E. D. Palik and J. K. Furdyna, Rep. Prog. Phys. **23**, 1193 (1970).

[4]R. S. Brazis, J. K Furdyna, and J. K. Pozela, Phys. Status Solidi A **53**, 11 (1979); **54**, 11 (1979).

[5]R. T. Holm and J. K. Furdyna, Phys. Rev. B **15**, 844 (1977).

[6]D. P. Mullin, R. R. Galazka, and J. K. Furdyna, Phys. Rev. B **24**, 355 (1981).

[7]R. T. Holm, Ph.D. thesis, Purdue University, 1973.

[8]C. P. Slichter, in *Principles of Magnetic Resonance,* Vol. 1 of *Springer Series in Solid-State Sciences,* edited by M. Cardona, P. Fulde, and H. J. Queisser (Springer-Verlag, New York, 1978).

[9]A. Abragam, *The Principles of Nuclear Magnetism* (Oxford University Press, London, 1961).

[10]G. E. Pake and T. L. Estle, *The Physical Principles of Electron Paramagnetic Resonance,* 2nd ed., *Frontiers in Physics Series* (Benjamin, Reading, MA, 1973).

[11]R. E. Kremer and M. R. Tamjidi, J. Cryst. Growth **75**, 415 (1986).

[12]B. E. Bartlett, P. Capper, J. E. Harris, and M. J. T. Quelch, J. Cryst. Growth **46**, 623 (1979).

[13]S. Takeyama and R. R. Galazka, Phys. Status Solidi B **96**, 415 (1979).

[14]R. E. Kremer (unpublished).

[15]S. Nagata, R. R. Galazka, D. P. Mullin, H. Akbarzadeh, G. D. Khattak, J. K. Furdyna, and P. H. Keesom, Phys. Rev. B **22**, 3331 (1980).

[16]R. E. Behringer, J. Chem. Phys. **29**, 537 (1958).

[17]J. K. Furdyna, J. Vac. Sci. Technol. **21**, 220 (1982).

[18]J. K. Furdyna, Proc. Soc. Photo-Opt. Instrum. Eng. **409**, 43 (1982).

[19]J. Lambe and C. Kikuchi, Phys. Rev. **119**, 1256 (1960).

[20]K. Falkowski, Acta Phys. Pol. **32**, 831 (1967).

[21]R. E. Kremer, Ph.D. thesis, Purdue University, 1983.

[22]P. H. Zimmermann, D. Davidov, R. Orbach, L. J. Tao, and J. Zitkova, Phys. Rev. B **6**, 2783 (1972).
[23]R. S. Brazis and J. K. Furdyna, J. Appl. Phys. **48**, 4267 (1977).
[24]R. R. Galazka, S. Nagata, and P. H. Keesom, Phys. Rev. B **22**, 3344 (1980).
[25]J. E. Sansonetti, D. P. Mullin, J. R. Dixon, Jr., and J. K. Furdyna, J. Appl. Phys. **50**, 5431 (1979).
[26]R. E. Kremer and J. K. Furdyna, Phys. Rev. B **31**, 1 (1985).